Transport and Collective Dynamics in Suspensions of Confined Swimming Particles

Juan P. Hernandez-Ortiz, Christopher G. Stoltz, and Michael D. Graham*

Department of Chemical and Biological Engineering, University of Wisconsin-Madison, 1415 Engineering Drive, Madison, Wisconsin 53706-1607, USA

(Received 1 July 2005; published 10 November 2005)

Direct simulations of large populations of confined hydrodynamically interacting swimming particles at low Reynolds number are performed. Hydrodynamic coupling between the swimmers leads to large-scale coherent vortex motions in the flow and regimes of anomalous diffusion that are consistent with experimental observations. At low concentrations, swimmers propelled from behind (like spermatazoa) strongly migrate toward solid surfaces in agreement with simple theoretical considerations; at higher concentrations this localization is disrupted by the large-scale coherent motions.

DOI: 10.1103/PhysRevLett.95.204501 PACS numbers: 47.55.Kf

The collective dynamics of swimming particles are interesting and important for a variety of fundamental and technological reasons. For example, there is long-standing interest in the theoretical biology and nonlinear physics communities in the collective motions of groups of organisms such as flocks and herds. Central issues here include the mechanisms by which autonomous agents interact to exhibit emergent collective behavior and the properties of the resulting behavior. Another is the evolutionary significance of these collective motions and whether different modes of collective swimming are more evolutionarily favorable than others in various circumstances. Recently, researchers have begun to experimentally study the fluid motions that directly arise in suspensions of swimming microorganisms [1–5], finding a fascinating variety of phenomena including regimes of anomalous transport as well as spatiotemporally coherent fluid motion on scales much larger than the organisms. Furthermore, it has recently been experimentally demonstrated that mass transport in a microfluidic device can be enhanced by the presence of swimming microorganisms [4].

The present work employs direct simulations to improve our understanding of these experimental observations. Attention focuses on a minimal model of the swimmers that captures the dominant far-field hydrodynamics while keeping the structure of each swimmer very simple. This approach is taken for two reasons: first, it focuses attention on the ''universal'' long-range interactions without the complicating, computationally expensive, and nonuniversal details of swimmer shape and detailed mechanism of propulsion, and second, it allows for relatively rapid solution of the equations of motion, enabling simulations of large populations. These simulations clearly illustrate that hydrodynamic interactions alone are sufficient to yield complex collective dynamics in swimming particle suspensions.

Wu and Libchaber [2] have experimentally characterized correlated motions in 1%–10% suspensions of *E. coli* confined to a horizontally suspended ''soap film'' of thickness ~ 10 μm. The fluid displayed intermittent flows in the form of swirls and occasionally jets, with length scales of 10–20 μm; this is of the same order of the film thickness, but the film thickness was not varied so it is not known if that is what set the scale of the motions. The authors studied the transport of tracer particles suspended in the film—note that these particles were 4.5–10 μm in diameter, significantly larger than the bacteria. The mean-squared displacement $\langle \Delta r^2(t) \rangle$ of the particles displayed two distinct regimes, a short time regime with anomalous (superdiffusive) transport, where $\langle \Delta r^2(t) \rangle \sim t^{1.5}$, and a longer time regime where the transport was diffusive. The crossover time between the anomalous and classical diffusion regimes increased with increasing bacterial concentration, varying between 1 and 10 s as concentration increased from about 1%–10%. In related work, Soni *et al.* [3] studied the motion of a particle in an optical trap contained within a suspension of *E. coli*, at volume fractions up to 0.1. They found that the correlation time for the position of the trapped particle increased monotonically with cell concentration, reaching a value of 1.2 s for the most concentrated suspensions.

Goldstein, Kessler, and co-workers have experimentally studied cell-driven motions in droplets of suspensions of *Bacillus subtilis* [5]. In sessile drops, conventional bioconvection patterns form, driven by a Rayleigh-Taylor instability induced as the denser cells swim upward toward the free surface, where the oxygen concentration is high [6]. In pendant drops, where the flow is gravitationally stable, flow patterns are also observed, with a length scale of ~ 100 μm and a correlation time of 1–2 s. Dramatically enhanced tracer diffusion is also found. The authors conjecture that the origin of these patterns is hydrodynamic interactions. Mendelson *et al.* [1] describe quite similar patterns in a slightly different situation. Colonies of *B. subtilis* were grown on agar surfaces. When a drop of water was placed on a colony, cells immediately began to swim, forming ''whirls and jets'' that persisted until the water soaked into the agar.

Modeling of the collective dynamics of moving organisms has been performed at a number of levels. A number

of researchers have studied active agent models of moving groups of self-propelled particles: here each particle moves and interacts with its neighbors according to an *ad hoc* set of rules. A simple but rich model of this type was proposed by Vicsek *et al.* [7]. In this model, at each time step every particle moves a constant distance in the direction of its current orientation, and the orientation is updated so that it is the average of the orientations of its neighbors, plus a bit of noise. As the magnitude of this noise is changed, the system's behavior undergoes a transition from ordered to disordered motion. Grégoire and co-workers [8] found that this model was able to reproduce the main features of the experiments of Wu and Libchaber. A related approach was taken by Toner and Tu [9], who wrote down general field equations for a conserved quantity (number density of particles) and a nonconserved one (flux of particles). This model can exhibit various solutions, including ordered phases in which all particles move in the same direction and disordered ones with large fluctuations in number density.

Another field-theoretic approach, this time with a more direct connection to the problem of interest here, was taken by Simha, Ramaswamy, and co-workers [10]. In their theory, the number of particles is conserved, as is fluid momentum. The effect of the particles on the fluid as they swim is accounted for by including a dipole forcing term in the Navier-Stokes equations. (To leading order in the far field, a neutrally buoyant swimming particle is a force dipole.) A third, nonconserved field is the orientation field of the swimmers, which is treated in a way similar to phenomenological treatments of the director field in nematic liquid crystals. With this model, the authors predict that (1) oriented (''nematic'') suspensions of self-propelled particles at low Reynolds number are always unstable to long wavelength disturbances and (2) the number density fluctuations in this case are anomalously large: for a system with N particles, the scaled variance $\langle(\delta N)^2\rangle/N$ of the number of particles in a given volume diverges as $N^{2/3}$. (This divergence is reminiscent of the controversial Caflisch-Luke divergence prediction in sedimentation [11].) A similar model has been developed by Liverpool and Marchetti, in the context of solutions of filament–motor-protein mixtures [12]. Again, a uniform oriented state is predicted to be unstable.

The results obtained from the aforementioned studies are suggestive and intriguing. They show that simple models obtained from general arguments predict nontrivial spatiotemporal patterns in the dynamics of self-propelled particles. But even the models described last, which do incorporate the Navier-Stokes equations, are limited. They do not capture from first principles the details of the hydrodynamic interactions, they are limited to very large length scales (as they treat the particle phase as a continuum field), and there are too many free parameters for conclusive analyses beyond linear stability to be performed. In the present work, we avoid these limitations, performing and analyzing the first direct simulations of suspensions of model self-propelled particles at low Reynolds number.

Simulations are performed with a minimal swimmer model, shown in Fig. 1, that captures the leading order far-field effects of hydrodynamic interactions between swimmers without specifying in detail the structure of the swimmer or its method of propulsion. Each swimmer is simply a rigid, neutrally buoyant dumbbell comprised of two beads connected by a rigid rod of length ℓ. The orientation of each swimmer is denoted by a unit director vector $\mathbf{n}$. All the drag on the swimmer is concentrated on the two beads. The propulsion is provided by a ''phantom'' flagellum, which exerts a constant force of magnitude f in the $\mathbf{n}$ direction on one of the beads, and an equal and opposite force on the fluid. The phantom flagellum can either push or pull on the dumbbell; the ''pushing'' case corresponds to most spermatozoa and many other microorganisms, but the ''pulling'' case is also commonly found in nature [13]. In our model the parameter p characterizes the ''polarity'' of the flagellar force: if $p = 1$, the flagellum pushes the swimmer; if $p = -1$, it pulls. The results presented here are for $p = 1$. Some organisms, such as *E. coli*, execute a complex ''run-and-tumble'' motion, during which they change directions at random intervals. In the present model, we do not account for such organism-specific effects: in isolation in an unbounded domain each swimmer would move in a straight line with constant speed $v_{\mathrm{sw}} = f/2\zeta + O(\frac{a}{\ell})$, where ζ and a are the Stokes law friction coefficient and radius of each bead. Overall, the swimming motion exerts no net force on the fluid, so in the far field the swimmer appears to be a moving symmetric force dipole (stresslet) [6,10]. In general, the torque balance on the swimmer also needs to be considered. However, the leading order far-field flow due to the torques is weaker than the stresslet contribution, so in the present minimal model we neglect this effect.

We have performed direct simulations of the particle motions in suspensions of these simple swimmers confined to the gap between two planar surfaces, considering the situation where the swimmers interact *only* through the low-Reynolds-number hydrodynamics of the solvent. If the number density of swimmers is n, one can define an

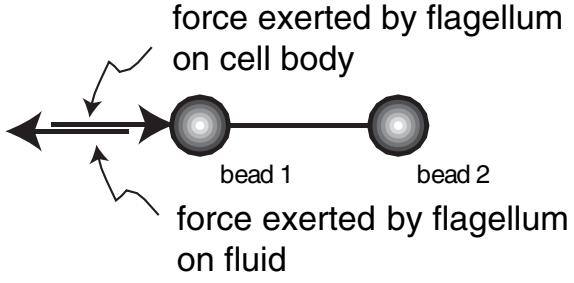

FIG. 1. Bead-rod-dumbbell model of a swimmer. The flagellum is represented by a force exerted on one of the beads of the dumbbell, and a force in the opposite direction exerted by the dumbbell on the fluid. The case $p = 1$ is shown.

effective volume fraction of particles in the suspension as $\phi_e = \pi n \ell^3/6$ [14]. Positions are nondimensionalized with ℓ and time with ℓ/v_{sw}. The domain is periodic with side L in the directions x and y parallel to the walls, and the distance between walls is $2H$. The force balance on bead 1 of each swimmer (neglecting inertia) is

$$\mathbf{F}_f + \mathbf{F}_{h1} + \mathbf{F}_{c1} = \mathbf{0}. \quad (1)$$

Here $\mathbf{F}_f$ is the force exerted by the flagellum on the bead and $\mathbf{F}_{c1}$ is the force that enforces the rigid rod constraint. The drag force $\mathbf{F}_{h1} = -\zeta[\dot{\mathbf{r}}_1 - \mathbf{v}'(\mathbf{r}_1)]$, where $\mathbf{r}_1$ is the position of bead 1 and $\mathbf{v}'(\mathbf{r}_1)$ is the fluid velocity induced at $\mathbf{r}_1$ by the motions of all the beads of all swimmers, as determined by solving Stokes' equation, treating each bead and flagellum as a point force. The equation of motion for bead 2 is analogous, except that no flagellum is attached to it. The hydrodynamic interaction computations (i.e., $\mathbf{v}'$ at the position of each bead) were performed using a fast ($N \log N$) method adapted [15] from Mucha *et al.* [16].

Figure 2 shows mean-squared displacement (MSD) in the xy plane vs time for swimmers and non-Brownian point particle tracers at two different concentrations, $\phi_e = 0.047$ and 0.233. At the lower concentration the transport is ballistic at short times, reflecting the straight-line swimming of an isolated particle. At longer times a crossover to diffusive behavior occurs, with the crossover time decreasing and the breadth of the crossover region increasing as concentration increases. At the higher concentration, the crossover region is more than a decade wide, indicating a region of apparently anomalous diffusion. The short- and long-time scalings of the MSD are independent of box size at constant concentration, as is the crossover time between regimes, but the actual values of the long-time diffusivities do indicate a dependence on the box size.

Figure 3 shows the effective long-time self-diffusion coefficient of swimmers and passive tracers as a function of ϕ_e for two different confinements. At low concentration, the effective diffusivity is high because the swimmers travel a long distance on a nearly straight path before the weak hydrodynamic fluctuations can significantly alter their trajectories. The flow is barely disturbed by the swimmers so tracers diffuse very slowly. As the concentration is increased the diffusivity of the swimmers decreases, as their naturally ballistic trajectories are increasingly perturbed by hydrodynamic interactions with other swimmers. Correspondingly, the naturally motionless tracers increasingly feel the motion of the swimmers, so their diffusivity increases. An important transition occurs around $\phi_e = 0.3$, where the diffusion coefficient of the swimmers begins to increase with increasing concentration, and diffusion of the tracers becomes comparable to that the swimmers. This reflects the emergence of strong large-scale coherent motions in the flow, driven by the collective motion of the swimmers. Figure 4 shows a snapshot of the velocity field generated by the swimmers in a suspension with $\phi_e = 0.56$ and $2H = 5$. It is very similar to velocity fields experimentally observed by Goldstein and co-workers [5]. From this plot it is apparent that the size of the flow structures is comparable to the wall separation $2H$.

One of the most important consequences of confinement of suspensions is that it can lead to migration of particles. It is well known that suspended droplets and polymer molecules move away from walls during shear flow [17,18]. The fundamental mechanism behind this phenomenon is that the stresslet flow induced by a point force dipole near a wall induces wall-normal motion at the position of the dipole [19,20]. A droplet or polymer molecule that has extended in a shear flow has a stresslet with polarity $p = -1$, which, when aligned parallel to a wall, leads to migration away from the wall. Conversely, a particle with a stresslet of polarity $p = 1$ (e.g., a swimmer pushed by its flagellum) will migrate toward the wall. Indeed a long-standing observation is that mammalian spermatozoa mi-

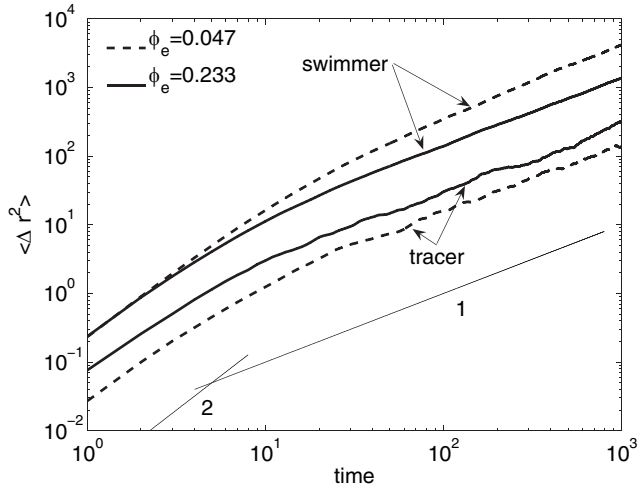

FIG. 2. Mean-squared displacement vs time for non-Brownian swimmer and tracer particles in suspensions of swimmers at various concentrations. $L = 15$ and $2H = 5$.

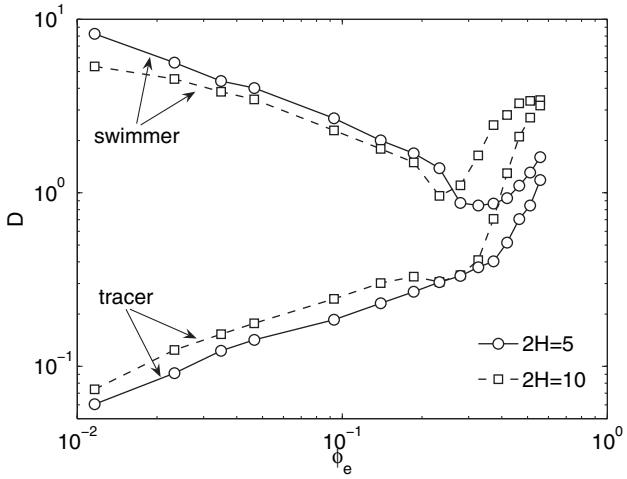

FIG. 3. Diffusion coefficient vs normalized concentration for the swimmer and tracer particles. $L = 15$.

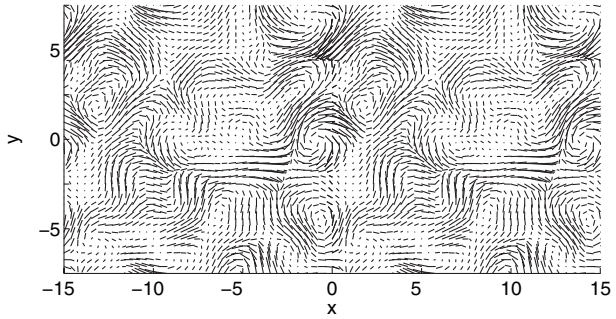

FIG. 4. Snapshot of the velocity field at the midplane of the channel for $\phi_e = 0.56$, $L = 15$, and $2H = 5$. Two periods in the x direction are shown, one in the y.

grate toward solid surfaces [21]. Rothschild [21] argued based on experiments that this effect is hydrodynamic, and detailed simulations of a single flagellated swimmer near a wall [22] predict motion of the swimmer toward the wall.

This motion is captured in our simple swimmer model. Figure 5 shows the concentration profile across the channel of swimmers at different average concentrations. As expected, at low concentrations the swimmers tend to move toward the confining walls, resulting in peaks in the concentration profile near the walls—the very low density at very small distances from the walls is simply due to the steric exclusion of beads from the walls. Once the concentration exceeds about $\phi_e = 0.3$, a quite important and unexpected phenomenon occurs: the sharp peaks near the wall vanish, as the emergent large-scale flow mixes fluid across the entire channel.

To summarize, many experimental observations of collective motion in suspensions of swimming particles can be captured by a very simple model of hydrodynamically interacting swimmers. The interacting particles display superdiffusive behavior at short time scales with a crossover to classical diffusion that is a function of concentration. At sufficiently large concentrations, large-scale coherent fluid motions emerge, leading to important changes in the transport within the system.

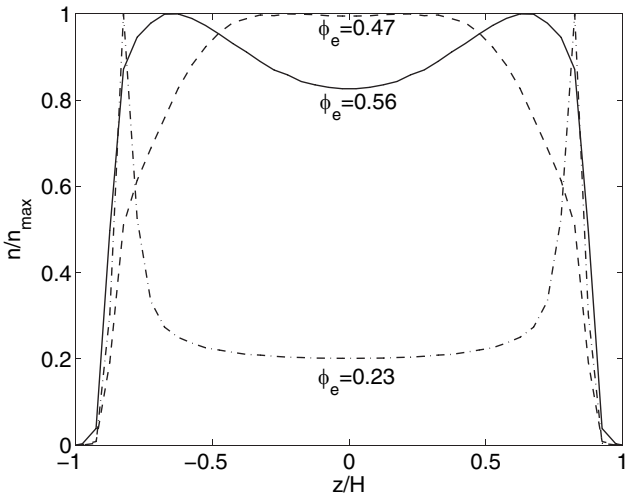

FIG. 5. Concentration profile as a function of wall-normal position z for different average concentrations. $L = 15$ and $2H = 5$.

This work was supported by the National Science Foundation, Grants No. DMR-0425880 and No. CTS-0522386, and a UW Grainger grant to C. G. S.

*Corresponding author.
Electronic address: graham@engr.wisc.edu

[1] N. H. Mendelson *et al.*, J. Bacteriol. **181**, 600 (1999).
[2] X.-L. Wu and A. Libchaber, Phys. Rev. Lett. **84**, 3017 (2000).
[3] G. V. Soni *et al.*, Biophys. J. **84**, 2634 (2003); Appl. Phys. Lett. **85**, 2414 (2004).
[4] M. J. Kim and K. S. Breuer, Phys. Fluids **16**, L78 (2004).
[5] C. Dombrowski, L. Cisneros, S. Chatkaew, R. E. Goldstein, and J. O. Kessler, Phys. Rev. Lett. **93**, 098103 (2004).
[6] T. J. Pedley and J. O. Kessler, Annu. Rev. Fluid Mech. **24**, 313 (1992).
[7] T. Vicsek, A. Czirók, E. Ben-Jacob, I. Cohen, and O. Shochet, Phys. Rev. Lett. **75**, 1226 (1995).
[8] G. Grégoire, H. Chaté, and Y. Tu, Phys. Rev. E **64**, 011902 (2001); G. Grégoire and H. Chaté, Phys. Rev. Lett. **92**, 025702 (2004).
[9] J. Toner and Y. Tu, Phys. Rev. Lett. **75**, 4326 (1995); Phys. Rev. E **58**, 4828 (1998).
[10] R. A. Simha and S. Ramaswamy, Phys. Rev. Lett. **89**, 058101 (2002); Y. Hatwalne, S. Ramaswamy, M. Rao, and R. A. Simha, Phys. Rev. Lett. **92**, 118101 (2004).
[11] R. E. Caflisch and J. H. C. Luke, Phys. Fluids **28**, 759 (1985).
[12] T. B. Liverpool and M. C. Marchetti, Europhys. Lett. **69**, 846 (2005).
[13] D. Bray, *Cell Movements: From Molecules to Motility* (Garland, New York, 2001), 2nd ed.
[14] Consistent with the conventions of the polymer and fiber suspension literature, we define an effective volume for each particle that is the size of a sphere of diameter ℓ. The dilute-semidilute crossover, above which steric effects become dominant, occurs when $\phi_e = O(1)$.
[15] J.-P. Hernandez-Ortiz, J. J. de Pablo, and M. D. Graham (to be published).
[16] P. J. Mucha *et al.*, J. Fluid Mech. **501**, 71 (2004).
[17] L. G. Leal, Annu. Rev. Fluid Mech. **12**, 435 (1980).
[18] U. S. Agarwal, A. Dutta, and R. A. Mashelkar, Chem. Eng. Sci. **49**, 1693 (1994).
[19] J. Smart and D. Leighton, Phys. Fluids A **3**, 21 (1991).
[20] H. Ma and M. D. Graham, Phys. Fluids **17**, 083103 (2005).
[21] Lord Rothschild, Nature (London) **198**, 1221 (1963).
[22] L. J. Fauci and A. McDonald, Bull. Math. Biol. **57**, 679 (1995).